Electron trajectories in rectangular antidot superlattices

S. Lüthi and T. Vancura

Solid State Physics Laboratory, ETH Zürich, 8093 Zürich, Switzerland

K. Ensslin

Solid State Physics Laboratory, ETH Zürich, 8093 Zürich, Switzerland;
Paul Scherrer Institute, 5232 Villigen PSI, Switzerland;
and Sektion Physik, LMU München, 80539 München, Germany

R. Schuster

Weizmann Institute, Rehovot 76100, Israel
and Sektion Physik, LMU München, 80539 München, Germany

G. Böhm and W. Klein

Walter Schottky Institut, TU München, 85748 Garching, Germany

A periodic array of potential pillars is superimposed on a two-dimensional electron gas being ballistic on the length scale of the lattice period. Pronounced maxima occur in the magnetoresistance of such systems. The magnetoconductivity as obtained from the magnetoresistance via a tensor inversion displays maxima or minima depending on the direction of current flow with respect to the lattice orientation. So-called pinned electron orbits as well as runaway trajectories coexist and specifically influence a given element of the conductivity tensor. In contrast to square lattices, both sets of trajectories show up in the experimental data simultaneously. [S0163-1829(97)02119-X]

I. INTRODUCTION

How is electron transport affected by a classical periodic potential? This question has been the focus of many recent experimental and theoretical publications. Here we will concentrate on so-called antidot lattices constituting a system with a periodic arrangement of potential pillars that exceed the Fermi energy in height. On the experimental side, hexagonal[1] as well as square[2] lattices have been fabricated and pronounced maxima have been observed in the magneto resistance.[3,4] These maxima have been attributed to the existence of pinned electron orbits around groups of antidots[5] leading to a reduced diffusion for magnetic fields, where the cyclotron diameter is commensurate with the lattice period. This intuitive interpretation has been complemented by so-called runaway trajectories[6] resembling skipping orbits along the rows of antidots thus predicting an enhanced diffusion. Diffusion is generally related to the conductivity via the Einstein relation rather than to the resistivity. By calculating the conductivities from the experimentally determined magneto-resistivities[7-9] it was shown that maxima as well as minima in the conductivity can occur at magnetic fields where the classical cyclotron diameter matches the lattice period. Quantum mechanically the miniband structure in an antidot potential was calculated[10] and successfully applied to interpret the experimental data.

Rectangular antidot lattices[11-16] also reveal maxima in the magnetoresistance whose position, however, depends on the direction of current flow with respect to the lattice orientation. Classical[17] as well as quantum-mechanical[18] calculations are in agreement with the experimental data. In particular it was shown that the observed anisotropy in the diagonal components of the resistivity tensor is related to the anisotropic miniband structure.[18] The importance of runaway trajectories in rectangular lattices was pointed out by calculating conductivities from the experimentally determined resistivities.[19]

Quantum oscillations superimposed on the classical commensurability oscillations have been observed in square lattices[20,21] and are explained by the quantization of periodic orbits around single antidots.[20,22,23] A quantum-mechanical calculation revealed the importance of the miniband structure and with it the density of states.[10,24] In finite structures smaller than the phase coherence length of the electrons, reproducible fluctuations superimposed on the classical commensurability maxima[12,25] are observed as well as Aharonov-Bohm-like oscillations.[25,26] The interpretation of these quantum effects relies fundamentally on pinned and therefore closed electron orbits. Quantum oscillations in the above sense of modified Shubnikov–de Hass (SdH) oscillations[22,23] were also detected in rectangular antidot lattices[16] and explained by the anisotropic miniband dispersion[18] in these systems.

In this paper we concentrate on the presentation of conductivity data for rectangular antidot lattices. In particular, we find that the conductivity along the wide open channels between the rows of antidots shows maxima each time the cyclotron diameter equals an integer multiple of the lattice period. For samples with small values of the lattice anisotropy the conductivity in the perpendicular direction, i.e., between the closely spaced antidots, displays minima. We conclude that runaway (maxima in the conductivity) and pinned (minima in the conductivity) electron trajectories influence the transport properties simultaneously. At very low mag-
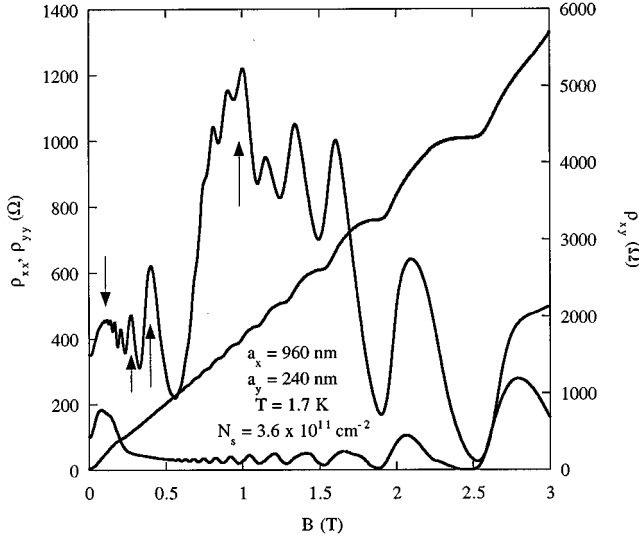
FIG. 1. Magnetoresistances and Hall resistance of a rectangular antidot lattice with a_x:a_y=4:1=960 nm:240 nm. The arrows pointing from below mark maxima in the magnetoresistance that are identified with the geometrical commensurability of the classical cyclotron diameter and the short lattice period a_y. The arrow pointing from above signifies a low-field maximum occurring in both ρ_{xx} and ρ_{yy} that is related to the scattering of the electrons as they travel in the open channels between the rows of the antidots.

FIG. 2. Magnetoresistance ρ_{xx} as a function of $2R_c/a_y$. The right part (scale on right-hand side) is the continuation of the same trace in an expanded scale. The features at $2R_c/a_y<1$ are Shubnikov–de Haas oscillations.

netic fields an additional maximum in the magnetoresistance is observed[12] being related to the boundary scattering in quantum-wire-like structures.[27] Here we show that this effect leads to a pronounced minimum in the conductivity along the wide open rows of antidots leaving the conductivity along the perpendicular direction unaffected.

II. SPECTROSCOPY OF CLASSICAL TRAJECTORIES

A high-mobility two-dimensional electron gas (2DEG) imbedded in an Al_xGa_{1-x}-As-GaAs heterostructure is patterned into an antidot lattice by electron beam lithography and a subsequent wet etching step. The details of the sample structure, the fabrication procedure, and the experimental setup are described in Ref. 12. In this paper we concentrate on two samples with lattice anisotropies of 2:1 and 4:1. Figure 1 shows typical magnetoresistance traces for an antidot lattice with a lattice anisotropy of 4:1. In the following, we identify the direction with the long lattice period with a_x and the short period with a_y. The magnetoresistivities ρ_{xx} and ρ_{yy} display a series of oscillations. At high magnetic fields, $B>2$ T where the classical cyclotron diameter at the Fermi energy

$$2R_c=2\frac{h}{e}\frac{\sqrt{2\pi N_S}}{B}$$

is much smaller than both lattice constants, SdH oscillations dominate the magnetoresistivities ρ_{xx} and ρ_{yy} and Hall plateaus show up in ρ_{xy}. Here N_s is the carrier density of the 2DEG. At low magnetic fields pronounced maxima occur in ρ_{xx}. The arrows pointing to the top in Fig. 1 mark magnetic-field positions where $2R_c=na_y$ with n=1,2,3. The addi-

tional low-field maximum marked by the arrow pointing to the bottom at $B\approx0.1$ T occurs from scattering at the rough edges in the wirelike geometry.[27] In order to resolve the classical commensurability oscillations more clearly, ρ_{xx} is plotted in Fig. 2 as a function of $2R_c/a_y$. Integers n along this axis resemble situations where the classical cyclotron diameter matches integer multiples of the short lattice constant. Up to n=7 the maxima of ρ_{xx} perfectly coincide with the vertical straight lines. Starting from n=8 the maxima become washed out and their positions deviate from the straight forward prediction.

In Fig. 3 circular orbits are plotted in a schematic antidot lattice with a_x:a_y=4:1. It is obvious from this simple geometric consideration that the orbit corresponding to n=8 is the first to touch the neighboring row of antidots and will therefore be deformed by the antidot potentials. This, however, will be true for both runaway trajectories (as sketched in Fig. 3) as well as for pinned orbits. In order to further
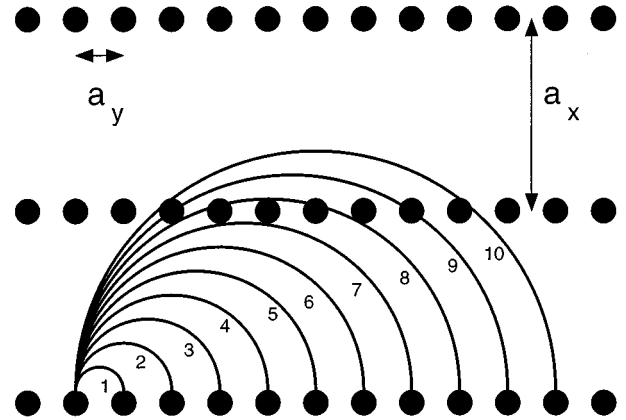
FIG. 3. Schematic trajectories with diameters na_y in a rectangular lattice with a_x:a_y=4:1.
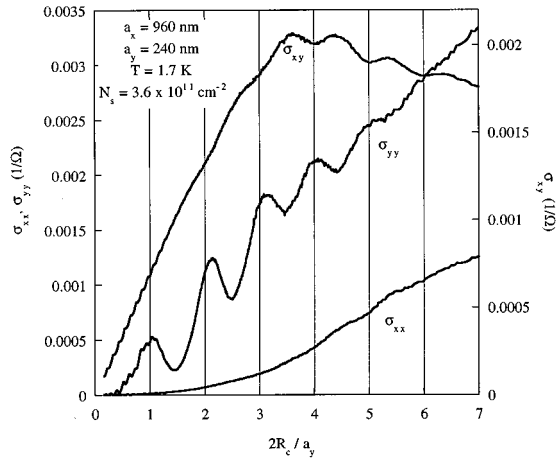
FIG. 4. Magnetoconductivities σ_{xx} and σ_{yy} (left-hand scale) and Hall conductivity σ_{xy} (right-hand scale) as a function of $2R_c/a_y$ for the same sample as in Fig. 1 with $a_x:a_y=4:1=960$ nm:240 nm.

understand the details of the characteristic trajectories we present data for the magnetoconductivities

$$\sigma_{xx}=\frac{\rho_{yy}}{\rho_{xx}\rho_{yy}+\rho_{xy}^2}, \quad \sigma_{yy}=\frac{\rho_{xx}}{\rho_{xx}\rho_{yy}+\rho_{xy}^2},$$

$$\sigma_{xy}=\frac{\rho_{xy}}{\rho_{xx}\rho_{yy}+\rho_{xy}^2}$$

in Fig. 4. The above formulas contain Onsager's relation $|\rho_{xy}|=|\rho_{yx}|$, which is supported by experimental data obtained on rectangular antidot.[11] It was shown theoretically[17] and experimentally[19] that the conductivity through the rows of antidots σ_{yy} is predominately related to the resistivity ρ_{xx} obtained for current flow through the closely spaced antidots. Here we investigate an antidot lattice with a larger anisotropy such that the influence of various kinds of trajectories is more pronounced due to the wide open space between the rows of antidots.

It is clear from Fig. 4 that σ_{yy} displays pronounced maxima at $n=1,2,3,4,5$. In the same magnetic-field range σ_{xx} and σ_{xy} are rather featureless (weak minima at $n=3,4,5,6$). The maxima in σ_{yy} are a clear signature of an enhanced conductivity related to runaway trajectories. These trajectories will hardly influence σ_{xx}. Since both runaway trajectories as well as pinned orbits oscillate periodically at least along one spatial coordinate they are expected to lead to minima in σ_{xy}. This is observed in the present case as well as in square lattices[7–9] for different parameter regimes.

In square lattices pinned orbits become more important for larger antidots. In this case pronounced minima occur in the conductivity at $2R_c=a$.[7,28] Furthermore quantum oscillations[20,21] as well as Aharonov-Bohm-like oscillations,[25] being explained on the basis of phase coherently closed orbits have been observed in systems with relatively large antidots. Quantum oscillations in rectangular lattices have been shown to be more pronounced for small lattice anisotropies.[16] In general the smaller the fraction of unperturbed electron gas in an antidot lattice, the more important are pinned orbits.
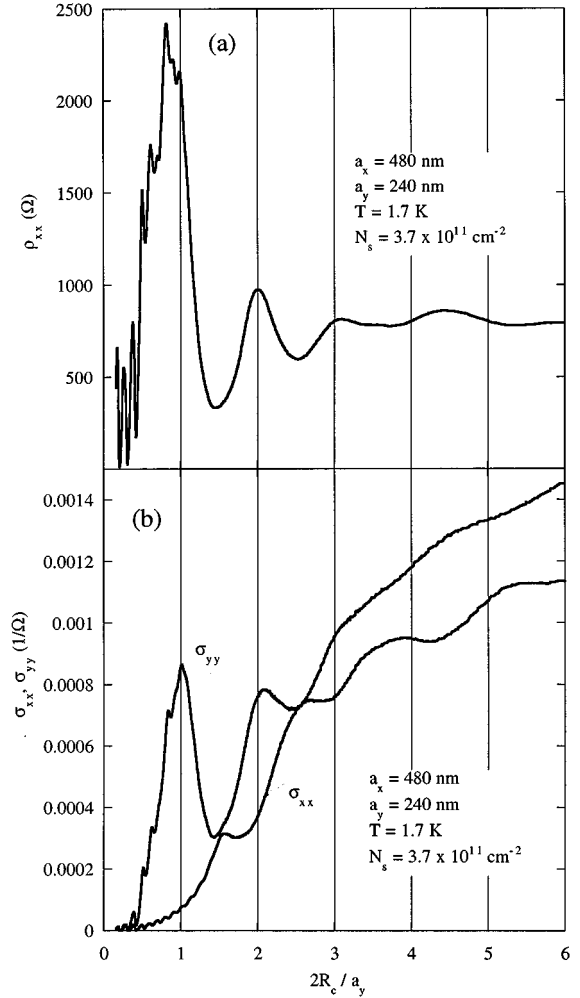
FIG. 5. Magnetoresistance ρ_{xx} (a) and magnetoconductivities σ_{xx} and σ_{yy} (b) for a sample with a small lattice anisotropy $a_x:a_y=2:1=480$ nm:240 nm.

Figure 5(a) presents the magnetoresistivity of a rectangular lattice with $a_x:a_y=2:1=480$ nm:240 nm as a function of $2R_c/a_y$. This smaller lattice anisotropy compared to the previous sample shows the transition to square lattices. Pronounced maxima occur in ρ_{xx} for $n=1,2,3$ while the position of the maximum for $n=4$ already deviates from the predicted position. This is expected from a sketch analogous to Fig. 3 where the orbit with a diameter of 4 small lattice constants should hit the neighboring row of antidots and is therefore expected to be deformed. Figure 5(b) shows the corresponding σ_{xx} and σ_{yy} traces for the same sample with $a_x:a_y=2:1=480$ nm:240 nm. As before σ_{yy} shows maxima at $n=1,2,3$.

The unexpected features occur in σ_{xx} where minima are observed at or close to $n=2,3,4$. Similar minima but much less pronounced can also be seen in Fig. 4 for σ_{xx}. These minima are interpreted as being related to pinned orbits around groups of antidots. At $n=2,4,6$ (for $a_x:a_y=2:1$) also runaway trajectories could occur along the x direction of the lattice. Since in the experiment clearly minima are observed in the conductivity σ_{xx} the influence of these orbits is not important. In this case of a lattice with anisotropy 2:1 we

have thus clear evidence that pinned orbits occur and have a significant influence on the conductivity in the respective conductivity direction between the closely spaced antidots.

This means that both kinds of trajectories, pinned (σ_{xx}) and runaway ($\sigma)_{yy}$, play a role in rectangular antidot lattices and can be analyzed via the components of the conductivity tensor. By comparing rectangular lattices with different degrees of anisotropy we find in agreement with geometrical considerations that pinned orbits become less important for lattices with larger anisotropies. This is consistent with the finding on square lattices where the importance of pinned orbits is hindered for small antidots leaving wide regions of unperturbed 2DEG. Furthermore it explains why a possible deviation of quantum oscillations from a $1/B$ periodicity becomes more significant for smaller anisotropies of the lattice periods.[16]

III. WIRELIKE EFFECTS IN RECTANGULAR LATTICES

At very low magnetic fields additional maxima show up in ρ_{xx} as well as in ρ_{yy} (see vertical arrow pointing from top in Fig. 1 at $B \approx 0.1$ T). These effects appear in rectangular lattices with large anisotropies[12] and are explained by the scattering of the electrons as they travel along the wide open regions confined by the rows of antidots similar as in quantum wires.[27]

In quantum wires one can measure a resistance or conductance. In our latticelike structures of dimensions that are much larger than the intrinsic length scales of the electronic system individual components of the resistivity or conductivity tensor can be obtained. Obviously the low-field maximum is observed in both diagonal components ρ_{xx} and ρ_{yy} of the resistivity tensor. In a plot of the corresponding conductivities σ_{xx} and σ_{yy} a similar feature is very difficult to discern since the Drude background is very steep in this low magnetic-field range. Therefore the conductivities have been fitted with a Drude-like expression which was subtracted thereafter, as has been done for square lattices.[7] A similar procedure was used for rectangular lattices with small lattice anisotropies $a_x : a_y = 1 : 0.8$ (Ref. 19) where this low-field maximum is not observed. Figure 6 shows the corresponding result for the sample with $a_x : a_y = 4 : 1 = 960$ nm:240 nm. While the σ_{xx} trace is rather featureless around $B \approx 0.1$ T the trace for the normalized σ_{yy} displays a pronounced minimum as marked by the arrow pointing from the top. The arrows pointing from below mark the maxima in the magnetoresistance that are related to $n = 1,2,3$.

Based on the Einstein relation which connects the diffusion constant with the conductivity, the identification of minima and maxima in the conductivity with certain electron trajectories leads to very sensible physical results. Furthermore, the original interpretation of the low-field magnetoresistance maximum is supported by this analysis.

IV. CONCLUSIONS

Experimentalists generally measure resistivities since this is the proper way to do a four-terminal experiment. Theo-
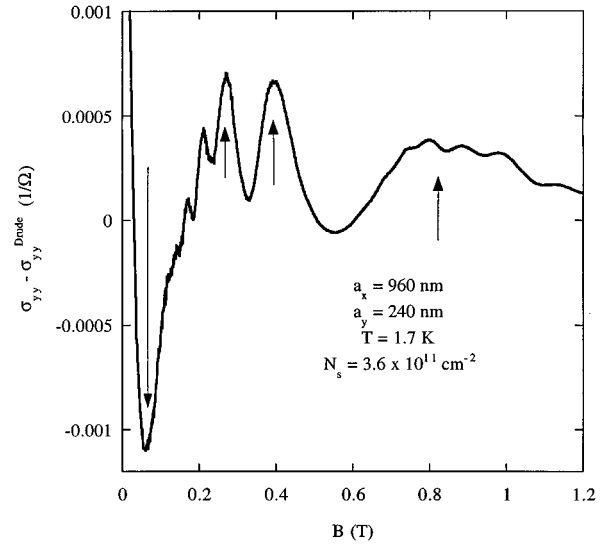
FIG. 6. Effective magnetoconductivity for the same sample as in Figs. 1 and 4. The data are obtained after a Drude fit to σ_{yy} has been subtracted from the original data. The arrows pointing from below mark geometrical commensurability conditions. The arrow pointing from above indicates the magnetic field, where a minimum occurs reflecting the enhanced scattering of carriers as they travel in the wide open channels between the rows of antidots.

rists, on the other hand, tend to calculate conductivities in the framework of linear response. Pronounced features have been experimentally found in the magnetoresistance of antidot superlattices and quantitatively explained by classical and quantum-mechanical calculations. While the conductivity is closely related to the rather intuitive diffusion constant the observed features are much more easily discernible in the resistivities. The open question remains whether conductivities and resistivities are related to different physical realities.

In this paper we demonstrate that the influence of pinned and runaway trajectories can be distinguished by evaluating the diagonal elements of the conductivity tensor. Furthermore we show that two different physical mechanisms, namely, boundary scattering in wirelike structures and the geometrical commensurability of the cyclotron diameter with the lattice constant, lead to minima and maxima, respectively, in the magnetoconductivity. It is a challenge for future experiments with smaller lattice period samples to test the general validity of these arguments in the quantum transport regime.

[1] H. Fang, R. Zeller, and P. J. Stiles, Appl. Phys. Lett. **55**, 1433 (1989); E. M. Baskin, G. M. Gusev, Z. D. Kvon, A. G. Pogosov, and M. Entin, Pis'ma Zh. Eksp. Teor. Fiz. **55**, 649 (1992) [JETP Lett. **55**, 679 (1992)].

[2] K. Ensslin and P. M. Petroff, Phys. Rev. B **41**, 12 307 (1990).

[3] A. Lorke, J. P. Kotthaus, and K. Ploog, Superlatt. Microstruct. **9**, 103 (1991).

[4] D. Weiss, M. L. Roukes, A. Menschig, P. Grambow, K. v. Klitzing, and G. Weimann, Phys. Rev. Lett. **66**, 2790 (1991).

[5] R. Fleischmann, T. Geisel, and R. Ketzmerick, Phys. Rev. Lett. **68**, 1367 (1992).

[6] E. M. Baskin, G. M. Gusev, Z. D. Kvon, A. G. Pogosov, and M. Entin, Pis'ma Zh. Eksp. Teor. Fiz. **55**, 649 (1992) [JETP Lett. **55**, 679 (1992)].

[7] R. Schuster, G. Ernst, K. Ensslin, M. Entin, M. Holland, G. Böhm, and W. Klein, Phys. Rev. B **50**, 8090 (1994).

[8] K. Ensslin and R. Schuster, in *Quantum Dynamics of Submicron Structures*, Vol. 291 of *NATO Advanced Study Institute*, edited by B. Kramer, H. Cerdeira, G. Schön (Kluwer Academic, The Netherlands, 1995), p. 247.

[9] D. Weiss, in *Quantum Dynamics of Submicron Structures* (Ref. 8), p. 327.

[10] H. Silberbauer and U. Rössler, Phys. Rev. B **50**, 11 911 (1994); H. Silberbauer, P. Rotter, M. Suhrke, and U. Rössler, Semicond. Sci. Technol. **9**, 1906 (1994).

[11] R. Schuster, K. Ensslin, J. P. Kotthaus, M. Holland, and C. Stanley, Phys. Rev. B**47**, 6843 (1993).

[12] R. Schuster and K. Ensslin, Festkörperprobleme **34**, 195 (1994).

[13] D. Weiss, K. Richter, E. Vasiliadou, and G. Lütjering, Surf. Sci. **305**, 408 (1994).

[14] K. Tsukagoshi, M. Haraguchi, K. Oto, S. Takaoka, K. Murase, and K. Gamo, Jpn. J. Appl. Phys. **34**, 4335 (1995).

[15] J. Takahara, A. Nomura, K. Gamo, S. Takaoka, K. Murase, and H. Ahmed, Jpn. J. Appl. Phys. **34**, 4325 (1995).

[16] R. Schuster, K. Ensslin, J. P. Kotthaus, G. Böhm, and W. Klein, Phys. Rev. B **55**, 2237 (1997).

[17] T. Nagao, J. Phys. Soc. Jpn. **64**, 4097 (1995).

[18] R. Neudert, P. Rotter, U. Rössler, and M. Suhrke, Phys. Rev. B **55**, 2242 (1997).

[19] K. Tsukagoshi, M. Haraguchi, S. Takaoka, and K. Murase, J. Phys. Soc. Jpn. **65**, 811 (1996).

[20] D. Weiss, K. Richter, A. Menschig, R. Bergmann, H. Schweizer, K. v. Klitzing, and G. Weimann, Phys. Rev. Lett. **70**, 4118 (1993).

[21] F. Nihey and K. Nakamura, Physica B **184**, 398 (1993).

[22] K. Richter, Europhys. Lett. **29**, 7 (1995).

[23] G. Hackenbroich and F. von Oppen, Europhys. Lett. **29**, 151 (1995).

[24] P. Rotter, U. Rössler, H. Silberbauer, and M. Surke, Physica B **212**, 231 (1995).

[25] R. Schuster, K. Ensslin, D. Wharam, S. Kühn, J. P. Kotthaus, G. Böhm, W. Klein, G. Tränkle, and G. Weimann, Phys. Rev. B **49**, 8510 (1994).

[26] K.-M. H. Lenssen, M. E. J. Boonman, C. J. P. M. Harmans, and C. T. Foxon, Phys. Rev. Lett. **74**, 454 (1995).

[27] T. J. Thornton, M. L. Roukes, A. Scherer, and B. P. Van de Gaag, Phys. Rev. Lett. **63**, 2128 (1989).

[28] K. Tsukagoshi, T. Nagao, M. Haraguchi, S. Takaoka, K. Murase, and G. Gamo, Superlatt. Microstruct. (to be published).